Crop Monitoring as an E-agricultural tool in Developing Countries

EVALUATION REPORT ON INTEGRATION OF RS DATA

Reference: *E-AGRI_D33.3_ Evaluation Report On Integration Of RS Data*
Author(s): Simone Bregaglio, Valentina Pagani, Giacinto Manfron, Mirco Boschetti, Roberto Confalonieri
Version: 1.0
Date: 10/01/2014

DOCUMENT CONTROL

Signatures

Author(s) : Simone Bregaglio
Valentina Pagani,
Giacinto Manfron
Mirco Boschetti
Roberto Confalonieri

Reviewer(s) :

Approver(s) :

Issuing authority :

Change record

Release	Date	Pages	Description	Editor(s)/Reviewer(s)
1.0	10/01/2014	28	D33.3 - Report	

TABLE OF CONTENT

LIST OF FIGURES

LIST OF TABLES

EXECUTIVE SUMMARY

This document reports on the evaluation of the accuracy of the BioMA models WARM and WOFOST in reproducing official yield statistics of rice in the Jiangsu province (China) using remotely sensed (RS) sowing dates and the maximum values of the Normalized Difference Vegetation Index ($NDVI_{max}$) to update the simulation of leaf area index (LAI). The BioMA models WARM and WOFOST were parameterized for rice within the activities reported in the E-AGRI report D32.3.

The simulated outputs in the period 2003-2010 were aggregated at the province level and then processed via the CGMS Statistical Tool Box to derive the yield forecasts. For each model, four simulation runs were performed: (1) without the assimilation of remotely sensed data, (2) forcing the model with the RS $NDVI_{max}$, (3) forcing the model with RS sowing dates, (4) forcing the model with RS $NDVI_{max}$ and sowing dates. The forecasts obtained with forced simulated indicators were compared to those derived by the BioMA-WARM and the BioMA-WOFOST models without the assimilation of exogenous data (option 1). Forecasting events were triggered in different moments during the crop cycle to assess the impact of RS data assimilation while the crop is approaching maturity.

The assimilation of RS sowing dates and $NDVI_{max}$ values into the BioMA-WOFOST and BioMA-WARM model determined a decided improvement of the accuracy in reproducing rice yield statistics in the Chinese Jiangsu province. On average, the BioMA-WOFOST model without forcing (R^2=0.769) obtained better results than BioMA-WARM (R^2=0.693). The only assimilation of RS $NDVI_{max}$ (option 2) determined an increase in the predictive ability of the two models, more pronounced for the BioMA-WOFOST model (R^2=0.825), whereas the assimilation of RS sowing dates (option 3) led the BioMA-WARM model to obtain the best improvements with respect to the simulations carried out without forcing (option 1). The combination of the assimilation of RS sowing dates and $NDVI_{max}$ led to the best results when the forecasting was carried out at DOY 260 and 280 (R^2 higher than 0.9), which correspond to the period in which most of the grid cells reached the $NDVI_{max}$ value. These tests were performed with simulations carried out at potential level, hence, the results obtained by the two models could be further improved by the combination of the assimilation of RS data with the simulation of the yield losses due to rice spikelet sterility and of blast disease, in order to increase the adeherence of the simulated system to the real one.

1. Introduction

The assimilation of remotely sensed (RS) information into crop growth models is an effective method to reduce the large uncertainty in the agro-meteorological, pedological and management data used as input for spatially distributed model applications (Aggarwal, 1995; Launay and Guèrif, 2005). The spectral profile of canopies retrieved from remote sensing provide timely qualitative and quantitative data on the evolution of the biophysical parameters referred to crop growth and development. This represents a clear advantage with respect to conventional field surveys, as it offers the potential for monitoring crop conditions across heterogeneous environments and over large areas (Bauer, 1975; Walburg et al., 1982).

The detection of rice cropped areas via remote sensing images can be more effective and efficient than for other crops, given the peculiarity of the agricultural management of paddy rice (Pei et al., 2011): after the preparation of the fields (e.g., plowing, harrowing and leveling), flooding irrigation is usually applied before sowing (or transplanting seedlings from a nursery bed). The crop cycle then develops through the vegetative and reproductive stages until harvest, with water present in the paddy at different depths during most of the season until draining prior to harvesting. The main applications of remote sensing for rice yield monitoring involve the crop detection, the paddy field mapping and the yield estimation or prediction (Park et al., 2013).

The new generation of advanced optical sensors, including the Moderate Resolution Imaging Spectroradiometer (MODIS) onboard the Terra and Aqua satellites provide shortwave infrared bands that are sensitive to vegetation moisture and soil water (Xiao et al., 2002). Different algorithms were developed using MODIS data to identify paddy rice fields, using the temporal profiles of the Normalized Difference Vegetation Index (NDVI) (e.g., Okamoto and Fukuhara, 1996; Okamoto and Kawashima; 1999; Van Niel et al., 2003; Boschetti et al., 2009; Manfron et al., 2012). NDVI is also one of the most used vegetation indices to derive rice leaf area index (LAI), via empirical relationships (e.g., Chen and Yang, 2005; Wang et al., 2007) or via bidirectional reflectance distribution function (BRDF) models (e.g., Roujean et al., 1992; Wanner et al., 1995). The former approach is widely adopted due to the small computation effort (Price and Bausch, 1995; Fassnacht et al., 1997; David et al., 1999).

In this report we evaluate the accuracy of the BioMA-WOFOST and of the BioMA-WARM models in reproducing rice official yields statistics in the Jiangsu province in the period 2003-2010, when RS sowing dates and NDVI data are used to force the two models. Spatially distributed simulations were carried out in the grid cells of the Chinese Jiangsu province and the outputs were aggregated and post-processed using the CGMS Statistical Tool Box to derive yield forecasts.

2. Materials and methods

2.1. Processing satellite data

The satellite data used to derive sowing dates and NDVI profiles in the Jiangsu province were the 16-day composite MODIS Surface Reflectance product MYD13Q1 (sensor: MODIS-Aqua) and MOD13Q1 (sensor: MODIS-Terra), downloaded from the United States Geological Survey (USGS) data base server (http://glovis.usgs.gov/). Every composite provides reflectance data on 4 spectral bands at 250-m spatial resolution, the bands are: b1-red (620-672nm), b2-near infrared (841-890nm), b3-blu (459-479nm), b7-medium infrared. This product type is derived from a multi-step process that consider atmospheric, clouds and aerosol corrections and accounts for each pixel the best reflectance data registered during the time composite window. The temperate rice cultivated areas in the Jiangsu province and the meteorological grid (spatial resolution 25×25 km) are shown in Figure 1.

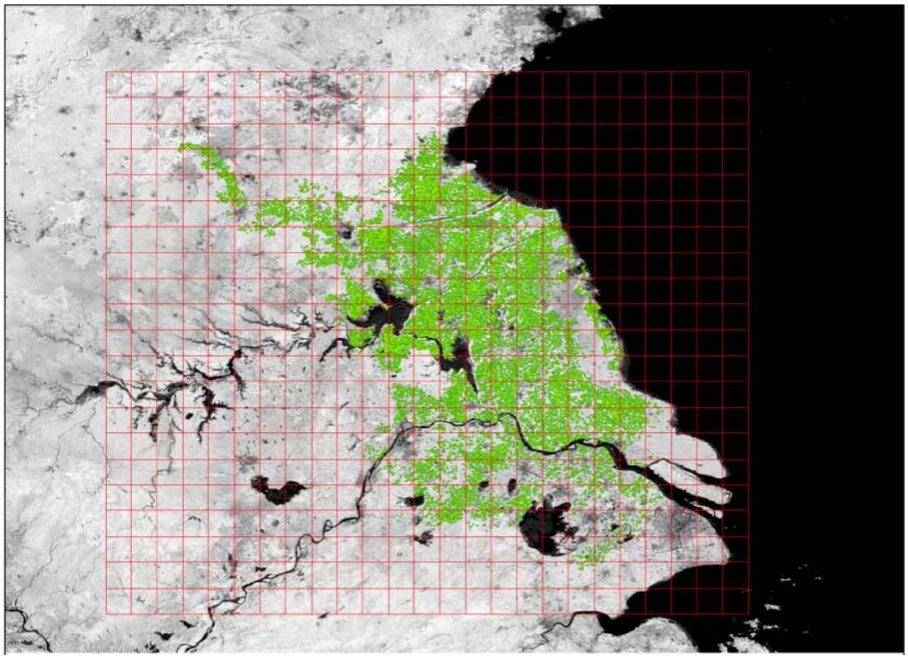

Figure 1: Rice cropped areas in the Jiangsu province and the meteorological grid (25×25 km) used to perform the simulations

The continuous temporal signal of spectral indices was processed by the PhenoRice algorithm (Manfron et al., 2012) to perform rice detection and rice seasonal monitoring.

This algorithm works with a rule based approach to identify rice when a clear flooding condition is detected, followed by a consistent and rapid crop growth.
Four steps are needed to complete the workflow: a) acquisition of RS data; b) data pre-processing to compute the noise and the NDVI spectral indices; c) smoothing of NDVI series via a polynomial function to reduce the impact of cloud contamination with a Savitzky-Golay filter (Luo et al., 2005); d) signal analysis and rice phenological detection. The main phenological stages of rice can be identified by the algorithm via different criteria. Four indicators are automatically computed (Figure 2, source Manfron et al., 2012): the day of year (DOY) of possible emergence (MIN), the early growing phase (Start of Season, SoS), the DOY in which maximum NDVI ($NDVI_{max}$) is reached (MAX, around heading) and a DOY close to the physiological maturity (End of Season, EoS).

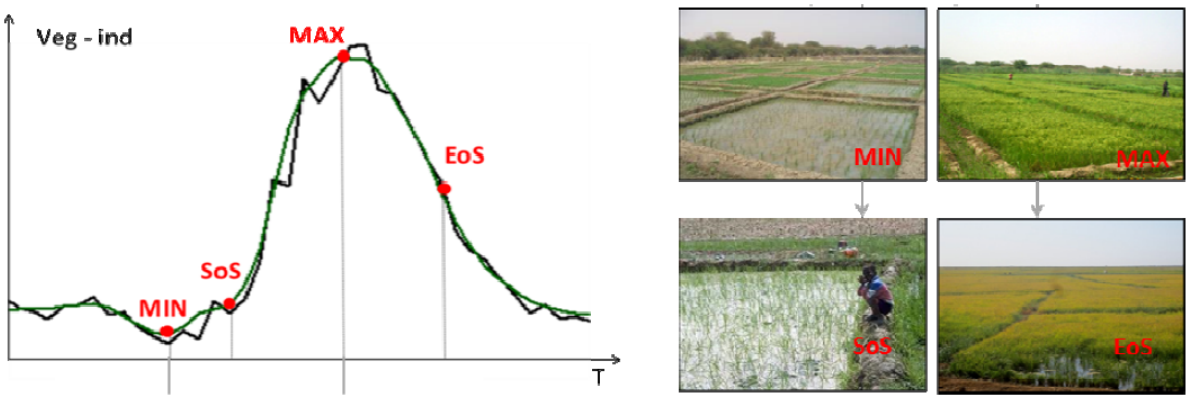

Figure 2: Timely occurrence and representation of phenological stages (MIN, MAX, SoS, EoS). Source Manfron et al. (2012)

Figure 3 shows an example of the NDVI profile and of the metrics that were extracted during the temporal series analysis: the green line represents a temporal series of NDVI data (real NDVI values were multiplied by 10^4 for computational purposes, y-axis). The example shows the identification of two crops during the analysed year, one in the second quarter and the other in the third quarter of the year.

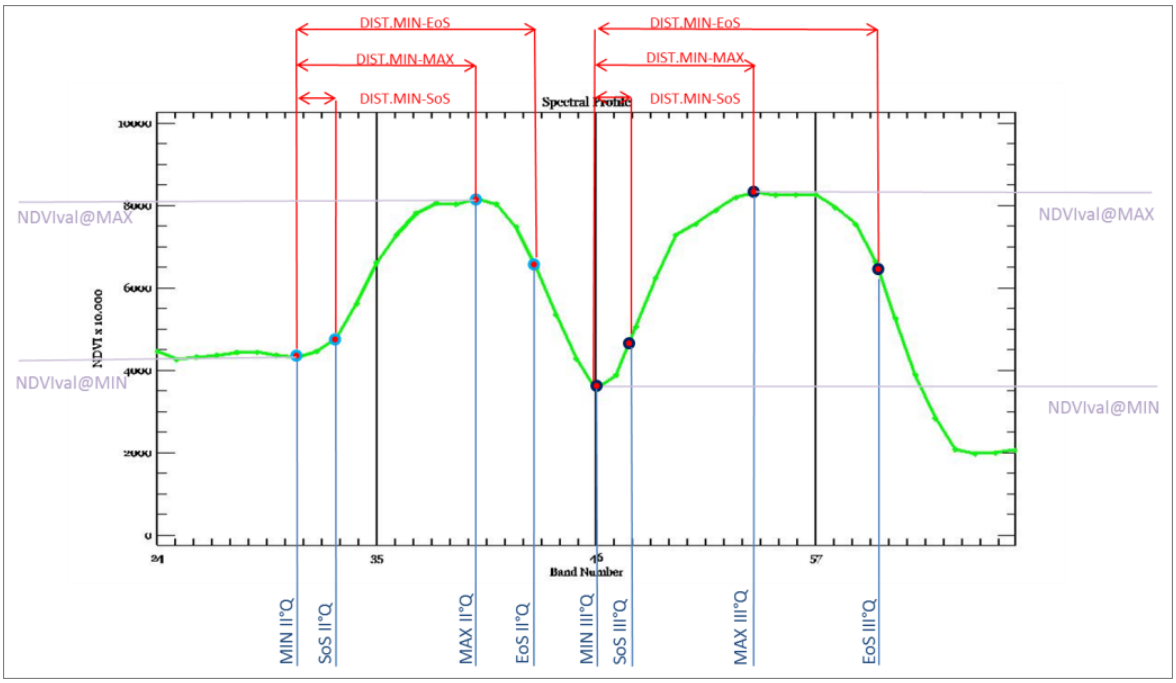

Figure 3: Example of a NDVI profile of one grid cell and one year under analysis, in which two crop cycles can be identified

For each grid cell in the Jangsu province and for each year, the RS indicators were computed and used to force the BioMA-WOFOST and the BioMA-WARM models.
In particular, the sowing DOY (in correspondence to the MIN indicator), and the DOY of occurrence of $NDVI_{max}$ and the $NDVI_{max}$ value were used (see paragraph 2.3). The RS data provider was the IREA-CNR (http://irea.cnr.it/).

2.2. Analysis of remotely sensed data

The total combinations of RS sowing dates and $NDVI_{max}$ data used to force the BioMA-WOFOST and BioMA-WARM models was 648 (81 grid cells × 8 years).
The box plots presented in Figure 4 and Figure 5 display the distributions of the $NDVI_{max}$ values and the corresponding days of the year in the period 2003-2010 in the Jangsu rice cropped area.

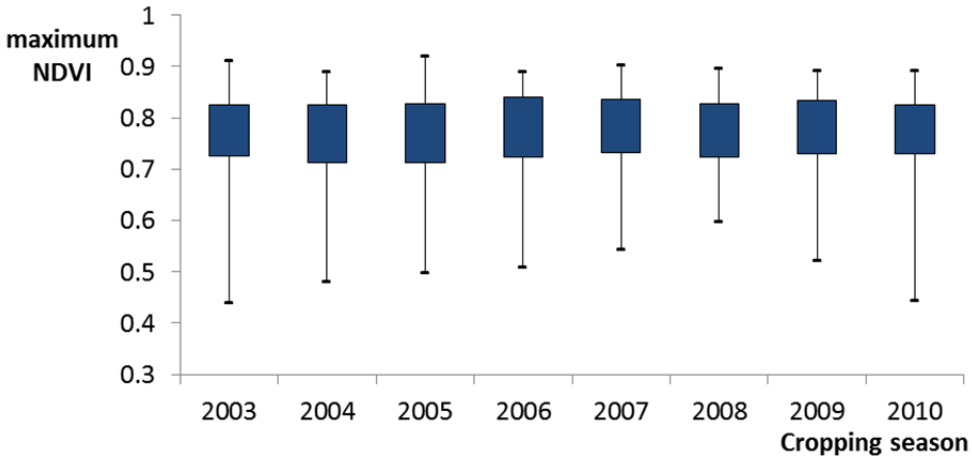

Figure 4: Boxplot showing the distributions of the maximum NDVI in the Jiangsu rice cropped area in the period 2003-2010.

The analysis of the distribution of the $NDVI_{max}$ values in the 2003-2010 cropping seasons highlights a very similar average value and heterogeneous distributions across the years, with 2008 presenting the smallest variability of $NDVI_{max}$ and 2003 and 2010 the highest one. The minimum value reached by $NDVI_{max}$ in the whole series is 0.437, whereas the maximum is 0.918.

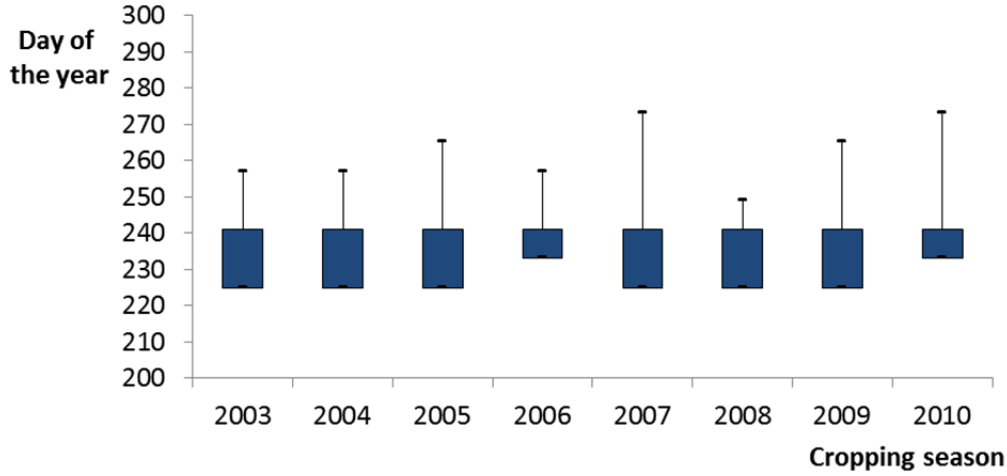

Figure 5: Boxplot showing the distributions of the day of the year in which maximum NDVI was reached in the Jiangsu rice cropped area in the period 2003-2010.

The analysis of the distribution of the DOY in which $NDVI_{max}$ is reached in the 2003-2010 cropping seasons highlights a constant minimum value (DOY 201) and very similar

distributions, except for 2006 and 2010 cropping seasons, which present less spread of data. The percentage of grid cells as a function of the DOY in which $NDVI_{max}$ is reached is shown in Figure 6. Since DOY 220, the number of grid cells is very low, then the maximum rate of increase is reached in the DOYs 230-250. After DOY 260, $NDVI_{max}$ is achieved in all the grid cells of the Jangsu rice cropped area.

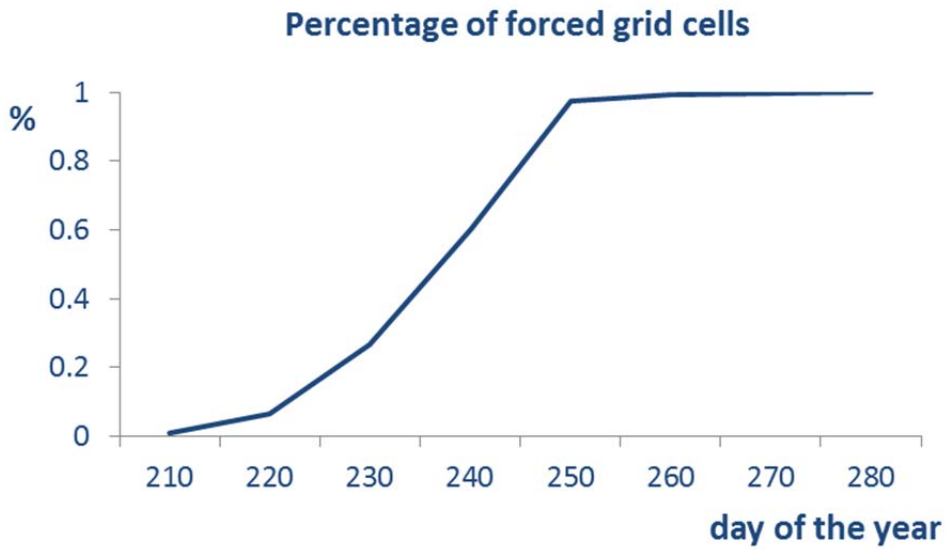

Figure 6: Percentage of grid cells in the Jangsu province in which $NDVI_{max}$ was reached as a function of time in the period 2003-2010 (source IREA-CNR data).

Figure 7 presents the distribution of the MIN indicator (used as a proxy of the sowing date, see paragraph 2.1.) in the Jangsu province during 2003-2010 cropping seasons.

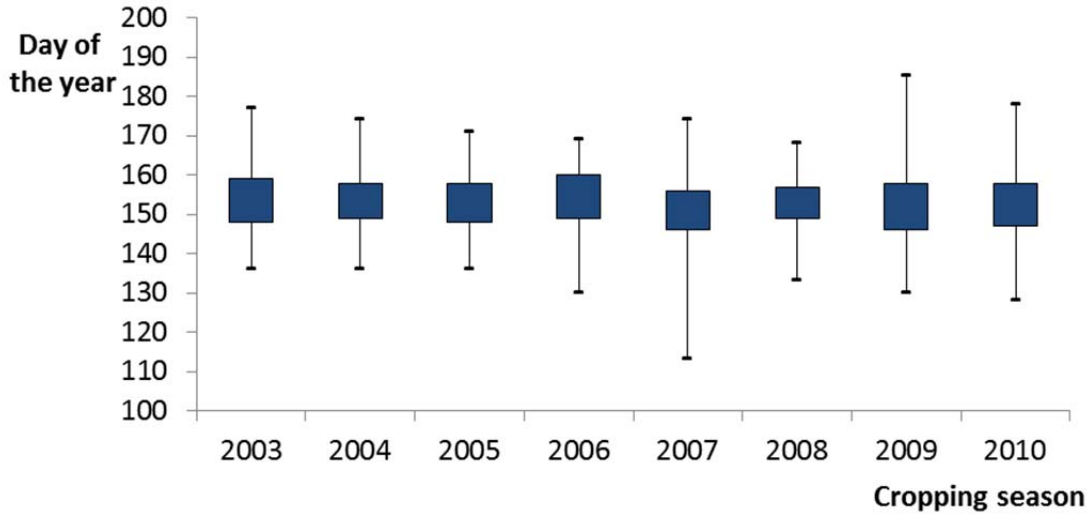

Figure 7: Boxplot showing the distributions of the sowing day retrieved from remote sensing in the Jiangsu rice cropped area in the period 2003-2010.

The analysis of the distribution of the RS sowing dates highlights a quite variable pattern across the years, with 2007 presenting on average the earliest sowing dates, with high variability across the Jangsu rice cropped area (minimum DOY=113, average DOY=151, maximum DOY=174). On the contrary, 2008 cropping season presents the smallest variability in the RS sowing dates (minimum DOY=133, average DOY=152, maximum DOY=168).

2.3. The NDVI-LAI empirical function

An empirical function (Wang et al., 2007) to derive rice LAI values from NDVI data (f_{NDVI_LAI}) was used to force the BioMA-WARM and the BioMA-WOFOST models. The NDVI-LAI relationship was developed starting from field data collected in an experimental farm of the Zhejiang University, Hangzhou, China (30°14' N, 120°10' E), which presents agrometeorological conditions similar to those experienced by rice in Jiangsu. Three rice varieties (Jiazao 324, Xieyou 9308 and Xiushui 110) were grown in 2002 and 2003 cropping seasons in a completely randomized design with four repeats. After the spectral measurements were carried out (ASD FieldSpe Pro FRTM, Analytical Spectral Devices), LAI of each plot was measured via a destructive method. An exponential relationship between LAI and NDVI (R^2=0.8563) was then found (Equation 1).

$$LAI = 0.1026e^{4.3892\,NDVI} \quad [1]$$

The plot of the f_{NDVI_LAI} function is shown in Figure 8.

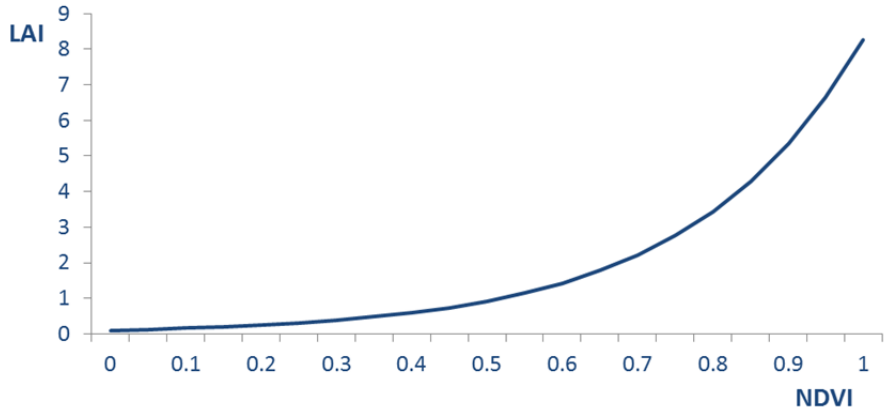

Figure 8: Leaf area index (LAI, m^2 m^{-2}) values computed as a function of NDVI with the empirical function developed by Wang et al. (2007)

This function was implemented in the UNIMI.Forcing component (see E-AGRI report D35.3). This component was then coupled with the BioMA-WOFOST and the BioMA-WARM models, both implementing a dynamic approach for daily partitioning of assimilates into leaves, stems and storage organs. The $NDVI_{max}$ was converted into LAI via the f_{NDVI_LAI} function and it was given as input to the BioMA-WOFOST and BioMA-WARM model in the corresponding DOY (Figure 9).

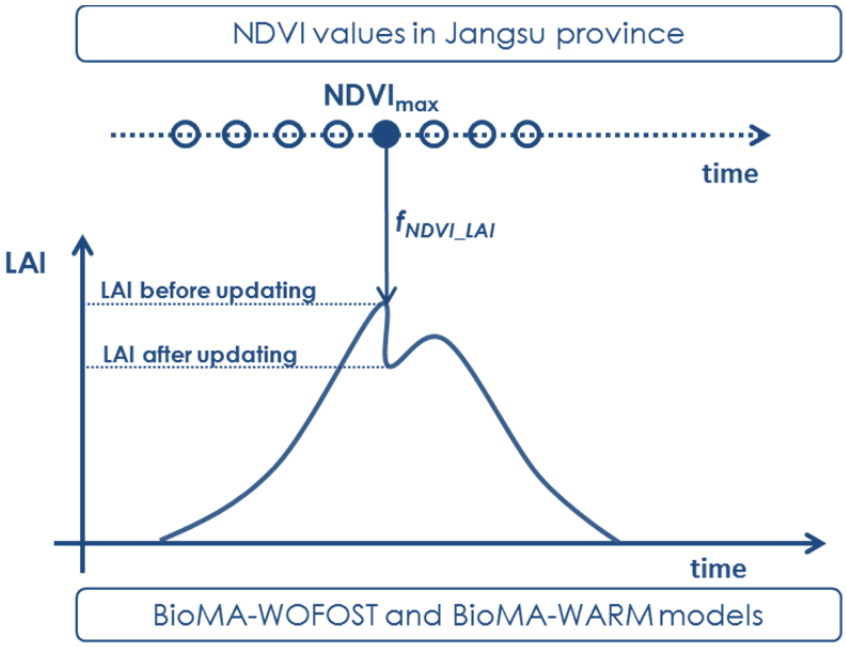

Figure 9: Schematic representation of the methodology adopted to force the BioMA-WOFOST and the BioMA-WARM models with LAI derived by $NDVI_{max}$ data.

After the forcing event and within the same model time step, the biomass of the plant organs (i.e., leaves, stems and storage organs) was derived from the new LAI value and from the updated specific leaf area (SLA, m^2 kg^{-1}).
The help and the code documentation files of the UNIMI.Forcing component are available at http://agsys.cra-cin.it/tools/.

2.4. Simulation experiment desing

A four-step simulation experiment design was defined to assimilate the RS data into the BioMA-WOFOST and the BioMA-WARM models (Figure 10). Each crop model was run in the Jiangsu rice cropped area in the period 2003-2010 (i) without the assimilation of RS data, (ii) by updating the LAI derived by the $NDVI_{max}$ value in the corresponding DOY; (ii) by assimilating the RS sowing dates (see paragraph 2.1), (iv), by combining the assimilation of RS sowing dates and $NDVI_{max}$ data.

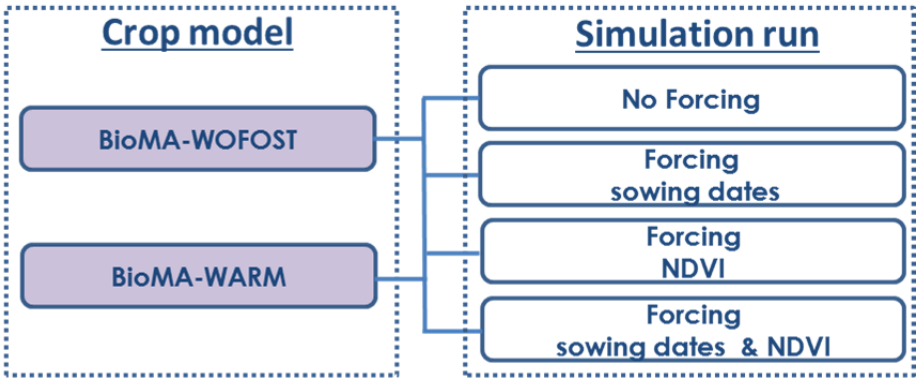

Figure 10: Simulation experiment design followed to evaluate the impact of the assimilation of remote sensing data into the BioMA-WOFOST and the BioMA-WARM model

For each simulation run, the outputs produced by the BioMA-WOFOST and BioMA-WARM models in each combination cropping season × grid cell were aggregated into decades to the Jiangsu province level using the CGMS database and then they were processed via the CGMS Statistical Tool Box to be compared with official yield statistics. The CGMS Statistical Tool Box is able to autonoumously select up to four model outputs (i.e., the indicators) to develop a multiple regression model using yearly official yields as dependent variable in different periods of the year (i.e., decades). The best regressive model (i.e., the one with the highest correlation index R^2 between simulated and official yields) obtained by each simulation run (i.e., no forcing, forcing with $NDVI_{max}$, forcing with RS sowing dates, forcing with RS sowing dates and $NDVI_{max}$) was chosen for the comparison. The forecasting were carried out at DOY 240, 260, 280, 300 and 320 in order to assess the impact of the forcing events during the crop cycle.

3. Results and Discussion

3.1. Analysis of the impact of forcing on time series of simulated outputs

The impact of forcing the two BioMA crop models with RS NDVI data markedly depends upon (i) the $NDVI_{max}$ value and (ii) the timing of the forcing event (DOY), as shown in Figure 11.

When the forcing event occurs after the peak of LAI (i.e., close to flowering stage) as in the grid cell 514 (year 2008), the impact on the aboveground biomass simulated by the BioMA-WOFOST (red lines) and the BioMA-WARM (blue line) models is very large. This is due to the combination of the low LAI value derived by the low RS $NDVI_{max}$ and by the late phenological stage: the simulated rice crop is in the ripening phase, therefore no new green leaf area is emitted because of the whole partitioning of the assimilates to the stems and panicles.

A different situation can be observed in the grid cell 4 (year 2003): even if the forcing event causes a reduction of LAI simulated by both the models, the impact in the accumulation of aboveground biomass is smoothed. In this case the simulated crop has time to produce new green leaves (especially according to the BioMA-WARM model), thus maintaining a close canopy stage (LAI around 3 m^2 m^{-2}) during a large part of the cycle.

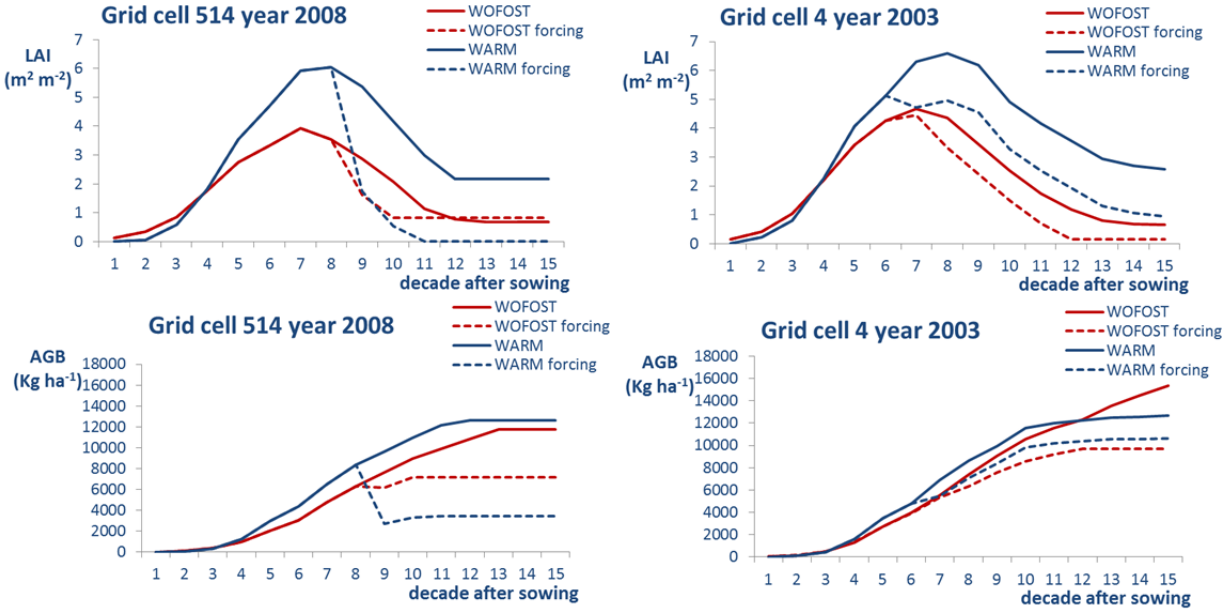

Figure 11: Simulations performed with the BioMA-WARM and the BioMA-WOFOST models in the grid cells 514 (year 2008) and 4 (year 2003). Comparison of the LAI and aboveground biomass accumulation without the updating of RS data and with the assimilation of $NDVI_{max}$.

Figure 12 shows the impact of the implementation of the sowing dates retrieved from remote sensing (see paragraph 2.1) on the evolution of LAI and aboveground biomass simulated by the BioMA-WARM (blue lines) and BioMA-WOFOST (red line) models. The anticipation of the sowing date determines higher and very similar LAI values for both the models, which in turns causes a higher accumulation of biomass with respect to the simulations carried out with a fixed sowing date (DOY 166). It can be noticed that the BioMA-WARM model computes a higher value of aboveground biomass than the BioMA-WOFOST one, even if the LAI values are similar.

On the contrary, the simulations performed with a fixed sowing date determine large differences in the LAI evolution patterns, leading to large dissimilarities in the simulated aboveground biomass, especially in the first-mid part of the crop cycle.

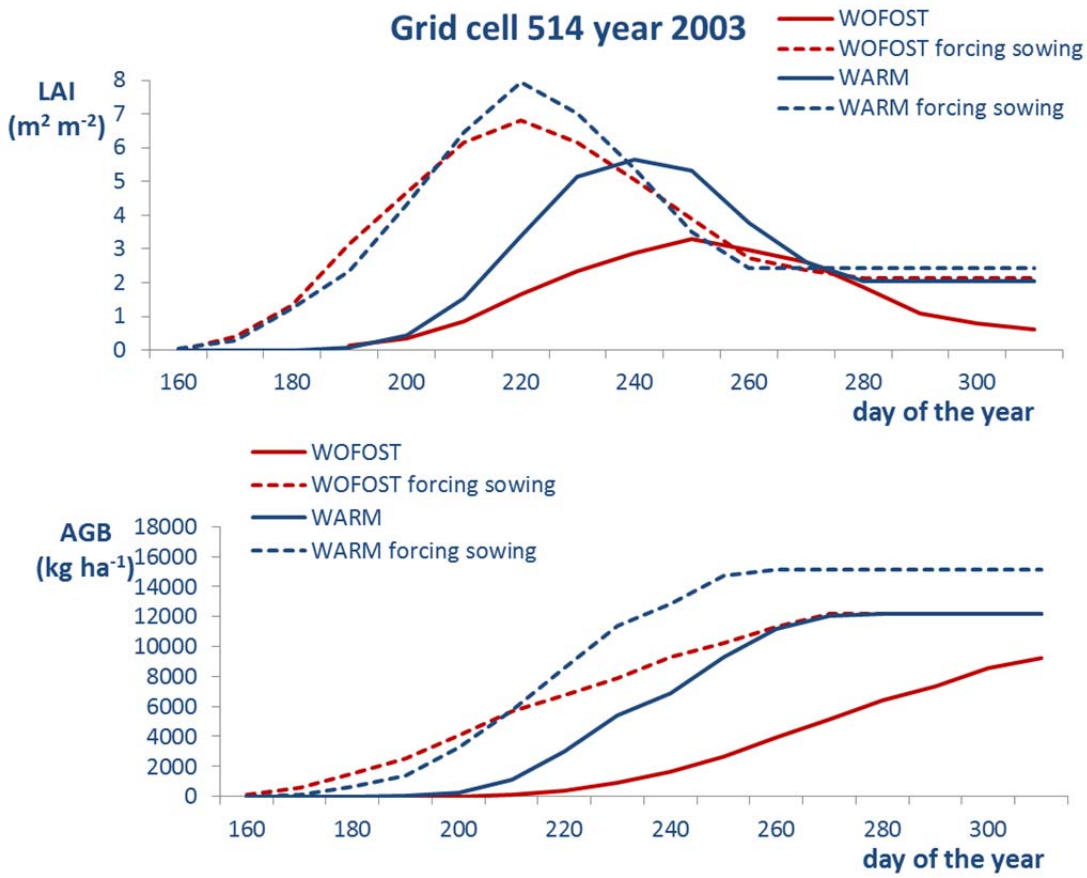

Figure 12: Simulations performed with the BioMA-WARM and the BioMA-WOFOST models in the grid cells 514 (year 2003). Comparison of the LAI and aboveground biomass accumulation by implementing the sowing date retrieved from remote sensing and a fixed sowing date (DOY 166)

Figure 13 shows the LAI and aboveground biomass accumulation simulated by the BioMA-WARM and the BioMA-WOFOST models in the grid cell 514 (year 2003). In the picture, the outputs of the four simulation runs (see paragraph 2.4.) are shown. The anticipation of the sowing date (i.e., retrieved from remote sensing) causes an increment in the accumulation of aboveground biomass for both the models. The forcing of the LAI values derived by $NDVI_{max}$ has a completely different impact according to the shift in the sowing dates. As already observed in Figure 10, when the sowing date is derived from remote sensing, it can be noticed a marked anticipation of the crop cycle. This in turns determines that the forcing event occurs very close to the flowering phase, thus causing a large impact in the accumulation of biomass. As a consequence, the simulations carried out without the implementation of the forcing event (i.e., highest aboveground biomass simulated with an anticipated sowing date) present an opposite pattern with respect to the ones in which

$NDVI_{max}$ is implemented, both for BioMA-WARM and BioMA-WOFOST models (i.e., highest aboveground biomass simulated with a delayed sowing date).

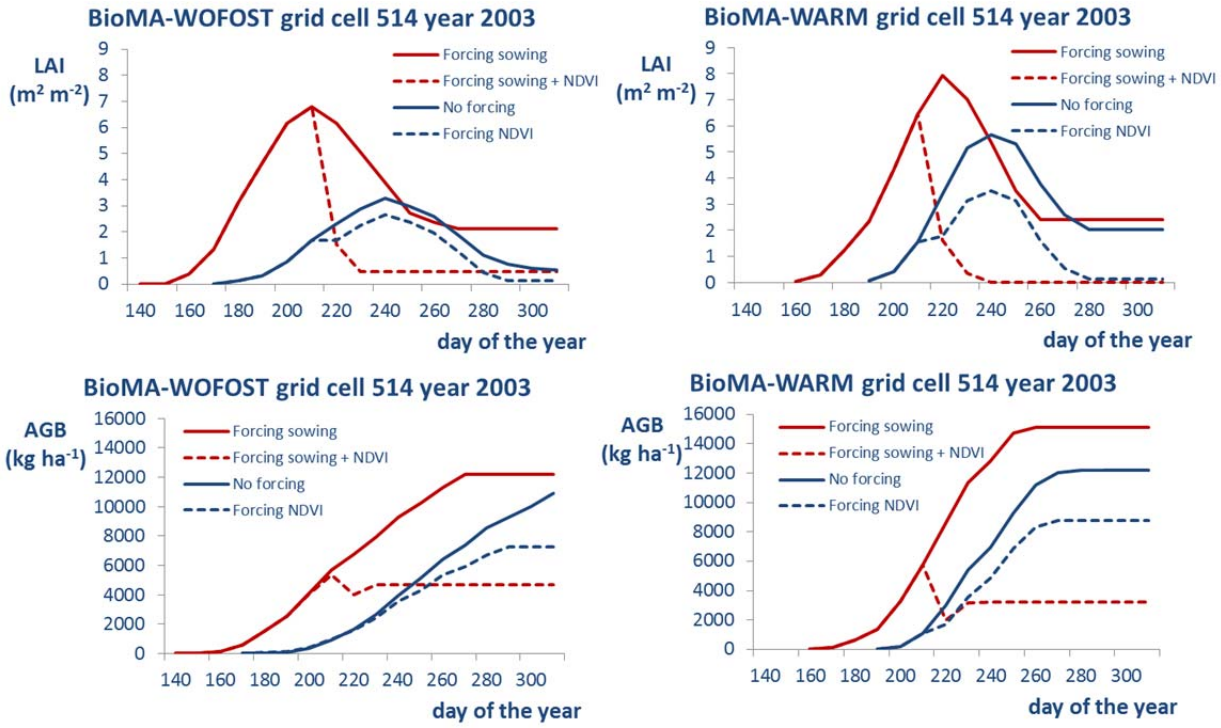

Figure 13: LAI simulations performed with the BioMA WOFOST model in the CGMS grid cell 31044 and year 2005. Comparison of the LAI trends without the updating of remotely sensed data and with the assimilation of maximum NDVI using the four functions tested.

3.2. Impact of the assimilation of remote sensing data in the forecasting system

The official yields statistics at the province level in Jiangsu (China) were used to evaluate the impact of the assimilation of RS data into the BioMA-WARM and the BioMA-WOFOST models. The coefficient of determination (R^2) between the official rice yield statistics and the yields computed by the multiple regressions with simulated outputs as predictors is reported in Table 1. The forecasting were carried out at DOY 240, 260, 280, 300 and 320.

Table 1: Correlation (R^2) values obtained by the multiple regression models with simulated outputs as predictors and official statistics. For each BioMA model (WARM and WOFOST), the four strategies of assimilation of RS data were applied. Forecasting of the official statistics was carried out in the period 2003-2010 at DOY 240, 260, 280, 300 and 32. Bold identifies the best result within the same DOY of forecasting.

Model	DOY	No Forcing	Forcing NDVI	Forcing sowing	Forcing sowing + NDVI
BioMA-WARM	*240*	0.653	0.613	0.938	**0.983**
	260	0.748	0.817	0.889	**0.947**
	280	0.552	**0.595**	0.534	0.583
	300	0.708	**0.810**	0.526	0.572
	320	0.806	0.760	**0.946**	0.808
BioMA-WOFOST	*240*	0.906	0.993	0.997	**0.999**
	260	0.817	0.902	0.746	**0.958**
	280	0.742	0.784	0.729	**0.900**
	300	0.704	0.749	0.719	**0.755**
	320	0.677	0.696	0.718	**0.736**

The correlation values obtained by the BioMA-WARM and BioMA-WOFOST models without the assimilation of RS data were never ranked 1st among the ones obtained by the three strategies used to force the models (see paragraph 2.4).

Considering the BioMA-WARM model, the only assimilation of RS $NDVI_{max}$ led to the best results in two out of five cases (i.e., forecasting carried out at DOY 280 and 300), as the combination of the assimilation of sowing dates and $NDVI_{max}$ (i.e., forecasting carried out at DOY 240 and 260). The correlation values obtained by the BioMA-WOFOST model clearly show the improvement due to the combination of the assimilation of RS $NDVI_{max}$ and sowing dates, as they are always the highest.

Figure 14 reports the average correlation values and the standard deviation computed between the values obtained by the BioMA models for the different forecasting decades.

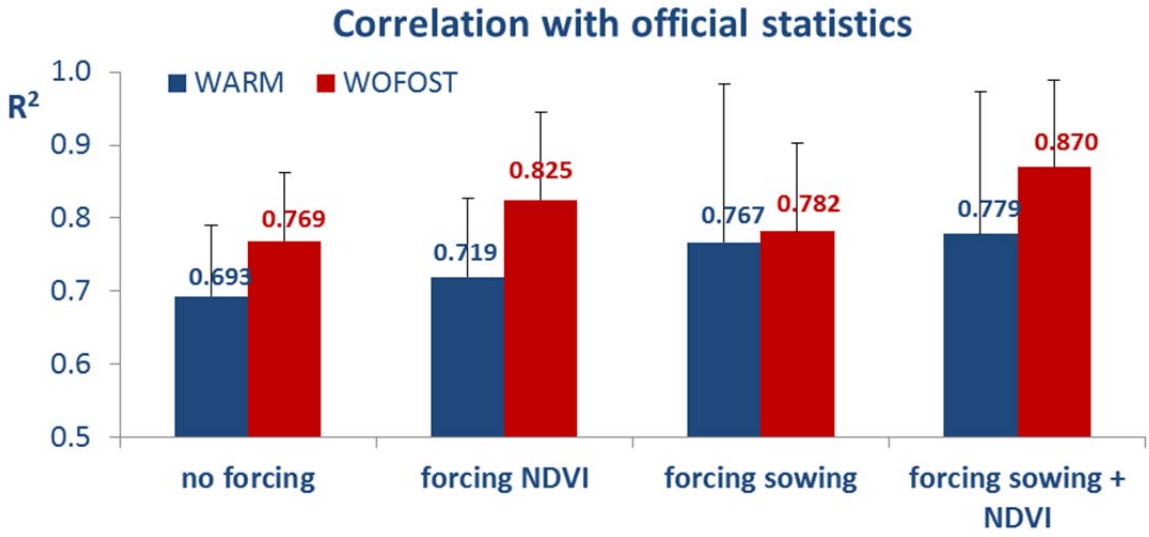

Figure 14: Average correlation (R^2) values obtained by the BioMA-WARM and the BioMA-WOFOST models in forecasting the official rice yield statistics in the Jiangsu province (China) in the period 2003-2010. The results obtained by the models without forcing and by the models forced with the different RS data assimilation strategies are shown.

On average, the BioMA-WOFOST model without forcing (R^2=0.769) obtained better results than BioMA-WARM (R^2=0.693). The only assimilation of RS $NDVI_{max}$ determined an increase in the predictive ability of the two models, more pronounced for the BioMA-WOFOST model (R^2=0.825). The assimilation of RS sowing dates caused an opposite situation: the accuracy of the two BioMA models increased, more markedly for the BioMA-WARM one (R^2=0.767). The combination of the assimilation of both sowinig dates and $NDVI_{max}$ determined a remarkable increase in the average correlation values obtained by the two models (R^2=0.775 for BioMA-WARM and R^2=0.870 for BioMA-WOFOST). Standard deviations computed between the DOYs of the forecasting (i.e., 240, 260, 280, 300 and 320) were higher when the assimilation of sowing dates was implemented, especially for the WARM model.

Figure 15 reports the official rice yield statistics in the period 2003-2010 in Jiangsu province compared with the predictions of the BioMA models in the DOY of forecasting in which the differences betweent the simulation runs (see paragraph 2.4) are maximized. It can be observed a remarkable improvement in the reproduction of the interannual fluctuations of rice yields for both the BioMA-models due to the implementation of RS data.

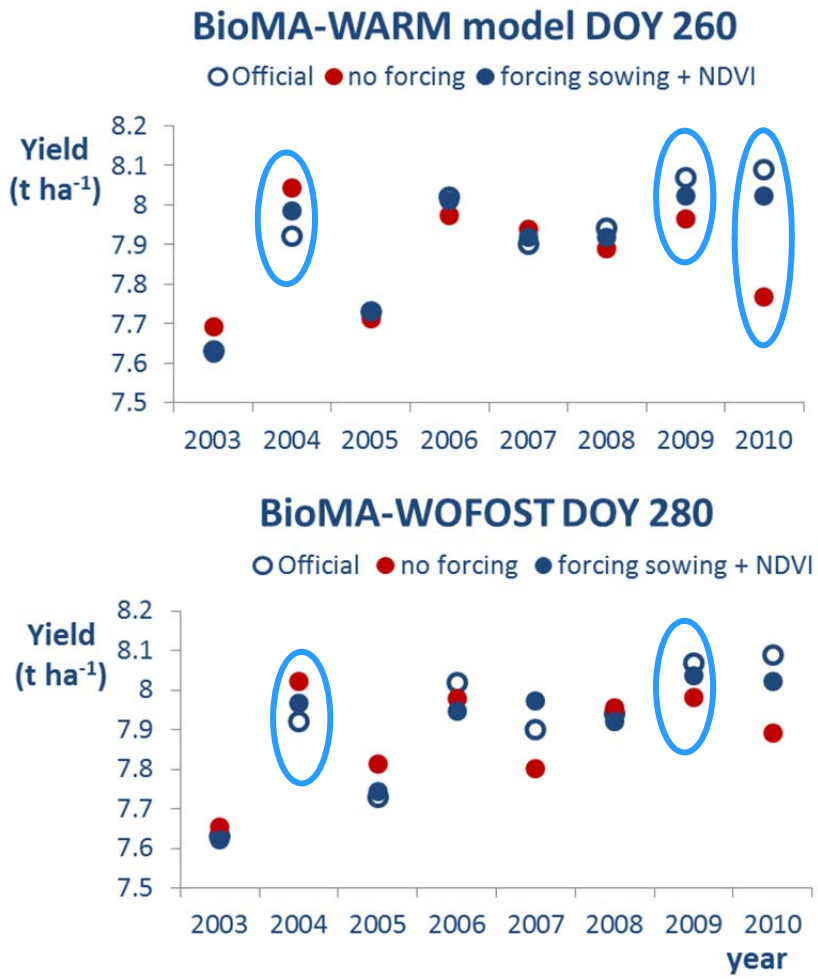

Figure 15: Official rice yield statistics (t ha^{-1}, empty circles)in the Jiangsu province in the period 2003-2010 compared with the predictions of the multiple regression built with the outputs of the BioMA models WARM and WOFOST without forcing (red circles) and with the assimilation of RS sowing dates and $NDVI_{max}$ (blue circles) in the DOY of forecasting in which the differences are maximized.

Figure 16 and Figure 17 reports the correlation values (R^2) obtained by the two BioMA models in each DOY of forecasting for the four simulation runs (see paragraph 2.4).

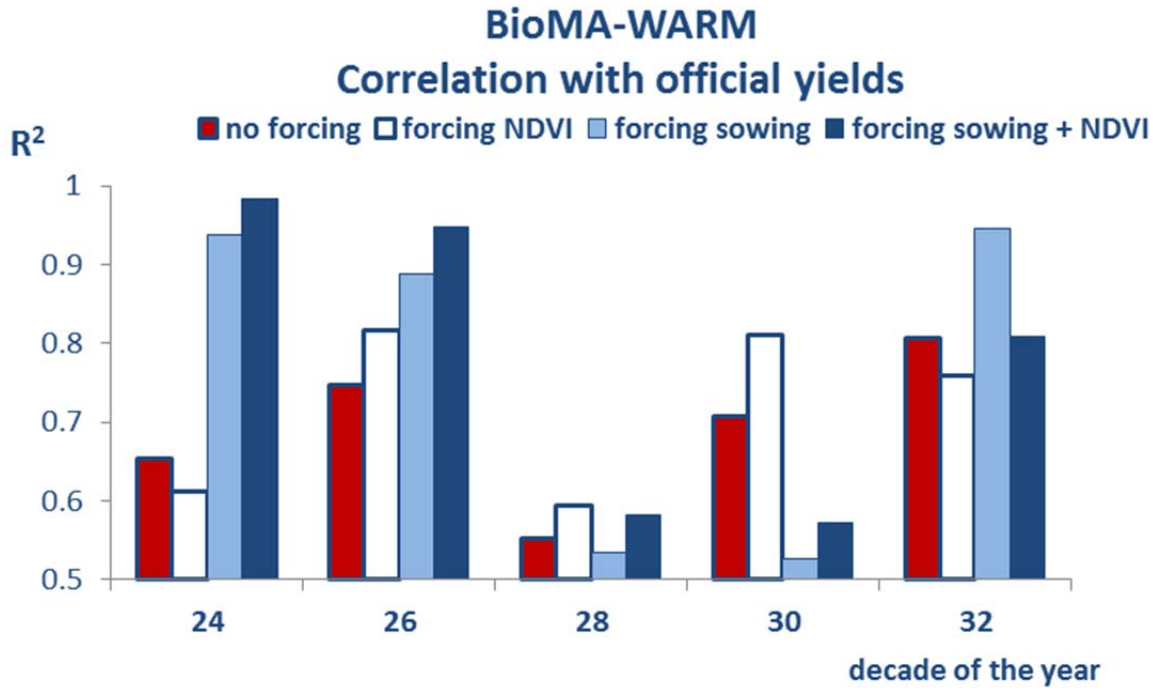

Figure 16: Correlation values (R^2) obtained by the regressive models using simulated outputs of the BioMA-WARM model as predictors between official rice yields statistics in the Jiangsu province (period 2003-2010). Forecasting were carried out at decades 24, 26, 28, 30 and 32. The four histograms refer to the four strategies of assimilation of RS data (i.e., no forcing, forcing with $NDVI_{max}$, forcing with RS sowing dates and forcing with RS sowing dates and $NDVI_{max}$)

At DOY 240, the impact of the assimilation of the only sowing dates allowed the BioMA-WARM model to obtain a considerable improvement in the prediction, whereas the only assimilation of $NDVI_{max}$ did not increase the correlation with official yields. The assimilation of RS sowing dates and $NDVI_{max}$ determined a remarkable increase in the accuracy of the prediction at DOY 240 and 260, in which the obtained R^2 values were very close to 1. This period corresponds to the maximum rate of increase of grid cells in which $NDVI_{max}$ was reached (Figure 6). The predictive ability of the BioMA-WARM model strongly decreased when the forecasting were made at DOY 280 and 300. At DOY 300, the best results were achieved by the simulation run in which only $NDVI_{max}$ was assimilated into the model. Close to physiological maturity (DOY 320), the performances of the multiple regressive models were quite similar and good, with the simulation run in which only sowing dates were assimilated obtaining the best result (R^2=0.946).

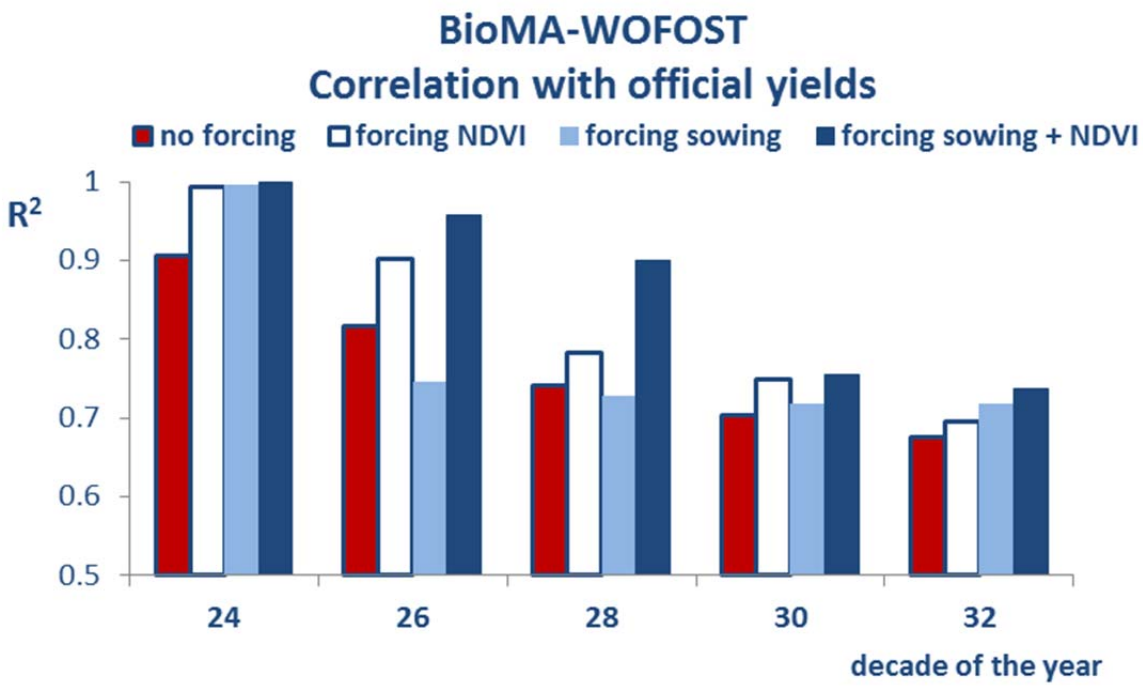

Figure 17: Correlation values (R^2) obtained by the regressive models using simulated outputs of the BioMA-WOFOST model as predictors between official rice yields statistics in the Jiangsu province (period 2003-2010). Forecasting were carried out at decades 24, 26, 28, 30 and 32. The four histograms refer to the four strategies of assimilation of RS data (i.e., no forcing, forcing with $NDVI_{max}$, forcing with RS sowing dates and forcing with RS sowing dates and $NDVI_{max}$)

It can be noticed a clear decreasing trend in the predictive ability of the multiple regressions built with the outputs of the BioMA-WOFOST model, according to the progress of the rice crop cycle. At DOY 240, the impact of the three strategies of assimilation of RS data was very similar and led to very good results (R^2 values were very close to 1). The impact of the assimilation of RS sowing dates and $NDVI_{max}$ allowed to maintain a high accuracy until DOY 280 (R^2=0.900), whereas the simulation run in which no assimilation of RS data was performed determined a steep decrease of the predictive ability (R^2=0.817 at DOY 260 and R^2=0.742 at DOY 280). At DOY 300 and 302 the performances of the four simulation runs were very similar and lower than the ones obtained by the WARM-model.

4. Conclusions

The assimilation of RS sowing dates and $NDVI_{max}$ values into the BioMA-WOFOST and BioMA-WARM model determined an overall remarkable improvement of the accuracy in reproducing rice yield statistics in the Chinese Jiangsu province in the period 2003-2010. The combination of the assimilation of RS sowing dates and $NDVI_{max}$ led to the best results when the forecasting was carried out at DOY 260 and 280, which correspond to the period in which most of the grid cells reached the $NDVI_{max}$ value. In general, the assimilation of the only $NDVI_{max}$ value (i.e., using a fixed sowing date) led to a lower improvement of the correlation between simulated and official yields than the assimilation of RS sowing dates. It can be noticed a decreasing trend in the predictive ability of the two models, especially for the BioMA-WOFOST one, when the forecasting is made during the ripening phase until physiological maturity. This is probably due to the lowering of the model ability in reproducing leaf area evolution after the implementation of the forcing event. Since only the potential level was simulated, without the consideration of the impact of biotic and abiotic stresses, this consideration cannot be considered as a general judgment of the models performances; conversely, it suggests to combine the assimilation of RS data with the simulation of the impact of rice spikelet sterility and of blast disease, in order to increase the adeherence of the simulated system to the real one.

5. References

Aggarwal, P.K., 1995. Uncertainties in crop, soil and weather inputs used in growth models: implication for simulated outputs and their application. Agricultural Systems 48, 361-384.

Bauer, M.E. 1975. The role of remote sensing in determining the distribution and yield of crops. Advances in Agronomy 27, 271-30.

Boschetti, M., Stroppiana, D., Brivio, P. A., Bocchi, S. 2009. Multi-year monitoring of rice crop phenology through time series analysis of MODIS images. International Journal of Remote Sensing 30, 4643-4662.

Chen, R.K., Yang, C.M., 2005. Determining the Optimal Timing for Using LAI and NDVI to Predict Rice Yield. Journal of Photogrammetry and Remote Sensing 10, 239-254.

David, P.T., Warren, B.C., Robert, E.K., Fassnacht, K.A., John, B.M. 1999. Relationships between leaf area index and Landsat TM spectral vegetation indices across three temperate zone sites. Remote Sensing Environment 70, 52-68.

Fassnacht, K.S., Gower, S.T., MacKenzie, M.D., Nordheim, E.V., Lillesand, T.M. 1997. Estimating the leaf area index of north central Wiscosin forest using the Landsat Thematic Mapper. Remote Sensing Environment 61,229-245.

Launay, M., Guèrif, M., 2005. Assimilating remote sensing data into a crop model to improve predictive performance for spatial applications. Agriculture, Ecosystem Environment 111, 321–339.

Liu, W.T., Kogan, F., 2002. Monitoring Brazilian soybean production using NOAA/AVHRR based vegetation condition indices. International Journal of Remote Sensing 2, 1161-1179.

Luo, J., Ying, K., Bai, J., 2005. Savitzky–Golay smoothing and differentiation filter for even number data. Signal Processing 85, 1429-1434.

Manfron G., Crema A., Boschetti M., Confalonieri, R. 2012. Authomatic procedures definition and validation to extract mapping and phenologicalrice fields informations through time series analysis of remote sensed MODIS data. Remote Sensing for Agriculture, Ecosystems, and Hydrology XIV, Proc. of SPIE 2012 paper number 8531-56.

Mo, X., Liu, S., Lin, Z., Xu, Y., Xiang, Y., McVicar, T.R., 2005. Prediction of crop yield, water consumption and water use efficiency with a SVAT-crop growth model using remotely sensed data on the North China Plain. Ecological Modelling 183, 301-322.

Okamoto, K., Fukuhara, M., 1996. Estimation of paddy rice field area using the area ratio of categories in each pixel of Landsat TM. International Journal of Remote Sensing 9, 1735-1749.

Okamoto, K., Kawashima, H., 1999. Estimating of rice-planted area in the tropical zone using a combination of optical and microwave satellite sensor data. International Journal of Remote Sensing, 5, 1045-1048

Park, J., Na, S., Park, J., 2013. Rice Growth Monitoring Model (RGMM) based on remote sensing techniques in South Korea. Global Journal on Advances Pure and Applied Sciences, 1. http://www.world-education-center.org/index.php/paas/article/view/2312.

Pei, Z., Zhang, S., Guo, L., McNairn, H., Shang, J., Jiao, X., 2011. Rice identification and change detection using TerraSAR-X data. Canadian Journal of Remote Sensing 37, 151-156.

Price, J.C., Bausch, W.C. 1995. Leaf area index estimation from visible and near-infrared reflectance data. Remote Sensing Environment 1995, 52, 55-65.

Roujean, J.L., Leroy, M., Deschanps, P.Y., A bidirectional reflectance model of the Earth's surface for the correction of remote sensing data, JGR-Biosciences, 97, 20455-20468 http://dx.doi.org/10.1029/92JD01411

Van Niel, T.G., McVicar, T.R., Fang, H., Liang, S., 2003. Calculating environmental moisture for per-field discrimination of rice crops. International Journal of Remote Sensing 24 885-890.

Van Keulen, H., Wolf, J., 1986. Modelling of agricultural production: weather soils and crops. Simulation Monographs. Pudoc, Wageningen, The Netherlands, pp. 479.

Xiao, X., Boles, S., Frolking, S., Salas, W., Moore, B., Li, C. et al., 2002. Observation of flooding and rice transplanting of paddy rice fields at the site to landscape scales in China using VEGETATION sensor data. International Journal of Remote Sensing 23, 3009-3022.

Xin, J., Zhenrong, Y., van Leeuwenb, L., Driessen, P.M., 2002. Mapping crop key phenological stages in the North China plain using NOAA time series images. International Journal of Applied Earth Observation and Geoinformation 4, 109-117.

Walburg, G., Bauer, M.E., Daughtry, C.S.T., Housley, T.L. 1982. Effects of nitrogen on the growth, yield, and reflectance characteristics of corn. Agronomy Journal 74,677-683.

Wang, F.M., Huang, J.F., Tang, Y.L., Wang, X.Z., 2007. New vegetation index and its application in estimating leaf area index of rice. Rice Science 14, 195-203.

Wanner, W., Li, X., Strahler, A.H., 1995. On the derivation of kernels for kernel-driven models of bidirectional reflectance, JGR-Biosciences 100, 21077-21090 http://dx.doi.org/10.1029/95JD02371.